DFT and experimental studies of the structure and vibrational spectra of curcumin

ARTICLE *in* INTERNATIONAL JOURNAL OF QUANTUM CHEMISTRY · MAY 2005

Impact Factor: 1.43 · DOI: 10.1002/qua.20469

4 AUTHORS, INCLUDING:

Tsonko Mitev Kolev
Bulgarian Academy of Sciences
214 PUBLICATIONS **1,640** CITATIONS
SEE PROFILE

Evelina Velcheva
Bulgarian Academy of Sciences
29 PUBLICATIONS **349** CITATIONS
SEE PROFILE

Bistra A. Stamboliyska
Bulgarian Academy of Sciences
47 PUBLICATIONS **623** CITATIONS
SEE PROFILE

DFT and Experimental Studies of the Structure and Vibrational Spectra of Curcumin

TSONKO M. KOLEV,[1] EVELINA A. VELCHEVA,[1] BISTRA A. STAMBOLIYSKA,[1] MICHAEL SPITELLER[2]

[1]*Institute of Organic Chemistry, Bulgarian Academy of Sciences, 1113 Sofia, Bulgaria*

[2]*Institute of Environmental Research, University of Dortmund, 44221 Dortmund, Germany*

Received 6 October 2004; accepted 5 November 2004
Published online 13 January 2005 in Wiley InterScience (www.interscience.wiley.com).
DOI 10.1002/qua.20469

ABSTRACT: The potential energy surface of curcumin [1,7-bis(4-hydroxy-3-methoxyphenyl)-1,6-heptadiene-3,5-dione] was explored with the DFT correlation functional B3LYP method using 6-311G* basis. The single-point calculations were performed at levels up to B3LYP/6-311++G**//B3LYP/6-311G*. All isomers were located and relative energies determined. According to the calculation the planar *enol* form is more stable than the nonplanar *diketo* form. The results of the optimized molecular structure are presented and compared with the experimental X-ray diffraction. In addition, harmonic vibrational frequencies of the molecule were evaluated theoretically using B3LYP density functional methods. The computed vibrational frequencies were used to determine the types of molecular motions associated with each of the experimental bands observed. Our vibrational data show that in both the solid state and in all studied solutions curcumin exists in the *enol* form.
 Int J Quantum Chem 102: 1069–1079, 2005

Key words: density functional theory; vibrational spectra; structure, band assignment

Introduction

The natural antioxidant curcumin [1,7-bis(4-hydroxy-3-methoxyphenyl)-1,6-heptadiene-3,5-dione] is the main constituent of the rhizomes of the plant *Curcuma longa L.* Curcumin has been used for a long time in the East as a dye, medicine, and flavoring. Nowadays, curcumin is becoming more and more popular due to its profound effect on human health [1]. Curcumin shows a remarkable range of pharmacological activity, including antioxidant, antiinflammatory, and anticancer activity [2–7]. It acts as a lypoxygenase substrate and also as an inhibitor of cyclooxygenase enzymes [8, 9]. Curcumin is considered to be a potential chemopreventive agent and has been clinically tested [10]. One of the most important factors considered to be responsible for

Correspondence to: T. M. Kolev; e-mail: kolev@orgchm.bas.bg
Contract grant sponsors: the DAAD, within the priority program "Stability Pact South-Eastern Europe," The Bulgarian National Fund of Scientific Research.
Contract grant number: X-1213.
Contract grant sponsor: Alexander von Humboldt Stiftung, Bad Godesberg, Germany (to Ts.K.).

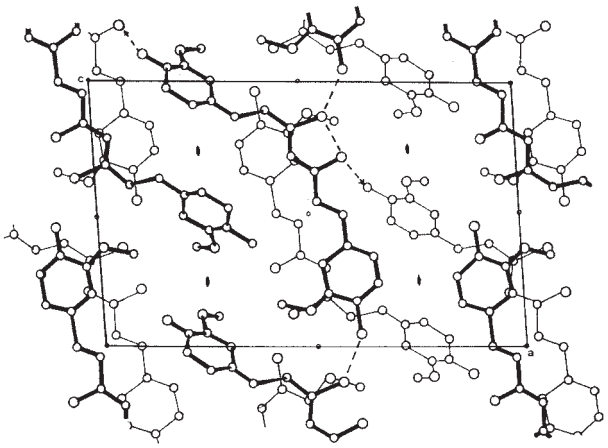

FIGURE 1. The molecular packing in crystal of curcumin.

the activity of curcumin is its ability to scavenge active oxygen or nitrogen-free radicals [6, 7, 11–13]. Some contradictory reports published in the last 5–6 years support two different antioxidant mechanisms. The investigations based on pulse radiolysis and other biochemical methods assigned the antioxidant activity to the phenolic –OH group [12–15]. In contrast, Jovanovic et al. [16, 17] showed that hydrogen abstraction from the methylene group is responsible for the remarkable antioxidant activity of curcumin. Both approaches regard only the diketo-form of curcumin. Detailed knowledge of the structure and spectral behavior of curcumin is an obligatory prerequisite for understanding its superb antioxidant activity. The most-used spectral method has been fluorescence spectroscopy [18, 19]. Much to our surprise, the vibrational spectrum of the titled compound has not been studied in detail. Miyamoto [20] published the IR spectrum of curcumin over a narrow spectral region and the bands observed were tentatively attributed. Tang et al. [21] investigated the supramolecular interaction of curcumin and β-cyclodextrin by electron absorbance, fluorescence, and IR spectroscopy. Schrader and colleagues [22] measured the FT Raman spectra of the extract from *Curcuma longa* roots and compared them with the spectra of the pure standard of curcumin without vibrational assignment. The crystal and molecular structure of curcumin was determined by single crystal X-ray diffraction by Tønnesen et al. [23] and is depicted in Figure 1. The molecule of curcumin crystallized centrosymmetrically in enol form. Electron delocalization and intramolecular hydrogen bonding in the crystal phase exist as the enol form is stabilized by a strong intramolecular H-bond. Moreover, this hydrogen bond appears invariably to be asymmetrical, the hydrogen atom always found to be bonded to one quince oxygen atom.

The molecular structure of curcumin, surprisingly, has not received the attention one might reasonably expect. We are aware of only one quantum chemical study [14] and we will refer to this study in the following discussion. Since the characterization of the most stable geometrical isomers of curcumin and the factors that contributed to their relative stability is essential to a complete understanding its biological properties, we used Density Functional Theory (DFT) in order to perform structural analysis of the diketo and enol forms of curcumin and to predict the infrared and Raman spectra of their relevant structural isomers. These results were then used to interpret the observed vibrational spectra for the studied molecule in solid state and in solution in order to correlate the structure with biological activity.

Theoretical and Computational Methods

All structures of the conformational isomers of curcumin were first optimized using DFT, which is a cost-effective method to approximate electron correlation effects. We employed the B3LYP functional, which combines Becke's three-parameter nonlocal exchange with the correlation functional of Lee, Yang, and Parr [24, 25], adopting a 6-31G* basis set without any symmetry restriction. For every structure, the stationary points found on the molecular potential energy hypersurfaces were characterized using standard analytical harmonic vibrational analysis. The absence of negative frequencies, as well as of negative eigenvalues of the second-derivative matrix, confirmed that the stationary points correspond to minima on the potential energy hypersurfaces. We also carried out single-point calculations with a larger basis set, 6-311++G**, to compute the total energies of the species studied.

The calculations of the fundamental vibrational frequencies and infrared and Raman intensities of the most stable enol and diketo forms were carried out at the B3LYP/6-31+G** level. For a better correspondence between experimental and calculated

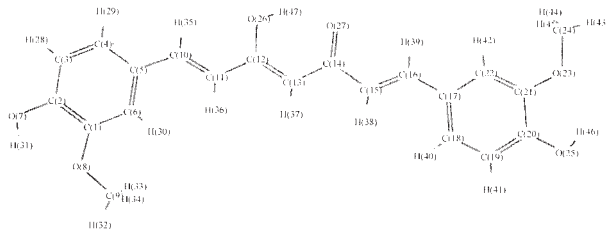

SCHEME 1. The most stable configuration of *enol* forms of curcumin.

values, we modified the results using the empirical scaling factors, reported by Scott and Radom [26]. All the calculations were carried out employing the Gaussian-98 program package [27]. In order to improve the visual representation of calculated IR spectra in the figures, the calculated absorption lines were replaced by Gaussian functions with a half-width of 10 cm^{-1}. The characterization of the modes reported was carried out by plotting the values of the displacement vectors obtained from Gaussian 98 output with the MOPlot program.

INFRARED AND RAMAN SPECTROSCOPY

Curcumin was obtained from Aldrich (Milwaukee, WI, purity 70%). In order to obtain product of high purity, preparative high-performance liquid chromatography (HPLC) was used. The product obtained under these conditions was an orange-red powder. The powder obtained was purified by recrystallization from ethanol to give suitable crystals for spectroscopic measurements. The compound was dissolved in the solvent at 70°C. Some drops of water were added to the solution and after 4 days in the refrigerator the deep-red crystals were separated by filtration (melting point, 182–183°C [23]).

The IR spectra were measured in solid state as KBr, CsI, and polyethylene pellets and in tetrachlormethane, chloroform, chloroform-D, and acetonitrile solutions on a Bruker IFS-113v FTIR spectrometer equipped with a high-intensity Globar source, Ge/KBr beam splitter, and DTGS detector in the middle infrared region. The cells were KBr, NaCl with 0.02–0.6 mm pathlength at a resolution of 1 cm^{-1} and 200 scans were used. The FTIR spectra were recorded with the same spectrometer using a high-pressure Hg arc lamp and a 6-μm Mylar beam splitter and DTGS detector. In all cases the spectra were recorded at a resolution of 1 cm^{-1} (200 scans). The Raman spectra were recorded for microcrystalline powder samples, introduced in capillary tubes at room temperature on a Jobin-Ivon 6400 spectrometer. The excitation was performed with 647.10 nm line laser in the 3500–50 cm^{-1} region using 50 mW powers.

Results and Discussion

CONFORMATIONAL ISOMERS OF CURCUMIN

In this article we report the structural, geometric, and conformational preferences of curcumin. It is well known that specific intramolecular interactions can stabilize different conformations. The presence of intramolecular hydrogen bonds between neighboring OH and OCH_3 groups has important implications regarding preferred molecular structures, as has been presented in the case of vanillin molecule [28]. We treat only these conformations. The keto and enol forms of the compound studied were optimized by means of the B3LYP/6-311G* basis set and the optimized structures are shown in Schemes 1 and 2. The method employed gave optimized structures almost perfectly planar for the enol form and nonplanar for the diketone form. This result differs from the published data [14]. In their DFT analysis, Priyadarsini et al. [14] computed a planar diketo structure. Our results suggest that that planar structure is 30.6 $kJ.mol^{-1}$ less stable than the nonplanar one. According to the B3LYP/6-311G* calculation, the most stable conformer of diketo form of curcumin can be regarded as composed of two nearly planar half-curcumin moieties setting up a torsion angle of 74° (Scheme 2). As is known, the β-dicarbonyl moiety assumes preferentially the planar *enol* form stabilized by the strong intramolecular H-bond, rather than the nonplanar *diketo* one. The energy difference between the keto and the enol configurations in this case amounts to ~20 $kJ.mol^{-1}$. Thus, we present only

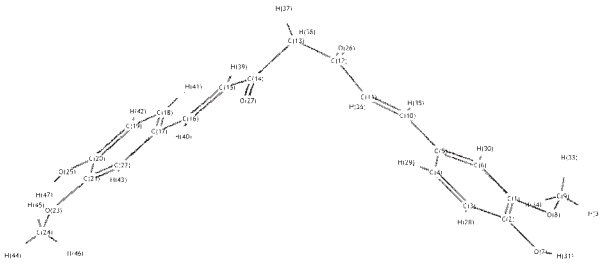

SCHEME 2. The most stable configuration of *diketo* forms of curcumin.

TABLE I

Total and relative energies of some curcumin isomers.

	B3LYP/6-31G*			B3LYP/6-311++G**// B3LYP/6-31G*	
Species	Total energy a.u.	VZPE kJ/mol	E_{rel} kJ/mol	Total energy a.u.	E_{rel} KJ/mol
E, E	−1263.5731275	976.666	0.00	−1263.94331246	0.00
E, Z	−1263.5653182	977.989	21.826	−1263.93516188	21.399
Z, E	−1263.5630266	977.218	27.072	−1263.93288993	27.364
Z, Z	−1263.5550267	978.791	49.648	−1263.92446816	49.475

the four possible planar geometric isomers with respect to the two double bonds of the molecule. In Table I we provide *E* and *Z* descriptors characterizing each structure, and these labels refer to the $C^{10}{=}C^{11}$ bond and $C^{15}{=}C^{16}$ bond, in that order. Optimized energies, vibrational zero-point energies (VZPE), and relative energies (E_{rel}) with respect to the most stable isomer are shown in Table I. As a result of these calculations we have found the E,E configuration to be the most stable (Table I). The relative energies, computed at B3LYP/6-31G* and at B3LYP/6-31++G**//B3LYP/6-31G*, are virtually the same.

Curcumin has four different rotation axes (two C—C single bonds and two C—Ph bonds) that can give rise to conformational isomers. The number of possible structures considered for optimization was 24. Some of these conformers are almost isoenergetic—we accept C_2 symmetry for the molecule. Under this assumption the number of possible conformers was reduced to nine and these are depicted in Scheme 3. We add the letter "a" and "b" to the structures to indicate two possible orientations of OCH_3 around C—Ph bond. The studied structures have *s-cis* and *s-trans* conformational orientations of C^{11}—H^{36} bond with regard to C^{12}—O^{26} and of C^{15}—H^{38} bond about C^{14}—O^{27}, respectively. The energies of the nine conformers of curcumin, optimized at the DFT(B3LYP)/6-31G* level, are represented in Table II. The most stable conformer (Scheme 1) of curcumin corresponds to the structure *a,s-trans,s-trans,b* and the energies of all other structures are given relative to the energies of this conformer. The other *s-trans,s-trans* structures are only slightly less stable, with E^{rel} lower than 1 kcal.mol^{-1}. On the other hand, all of the *s-trans,s-cis* isomers are significantly less stable, with E^{rel} ~10 kcal.mol^{-1}. The least stable are *s-cis,s-cis* structures with E^{rel} ~20 kcal.mol^{-1}. In the light of the above discussion, the structural distortions in conformer 1–9 can be recognized as a result of the balance between two driving forces: the H,H and H,O repulsions. In the case of the isolated molecule H,O and H,H, repulsions are overcome by means of a gain of resonance stabilization. In the cases of nonplanar conformers, no minima were found using the methods described.

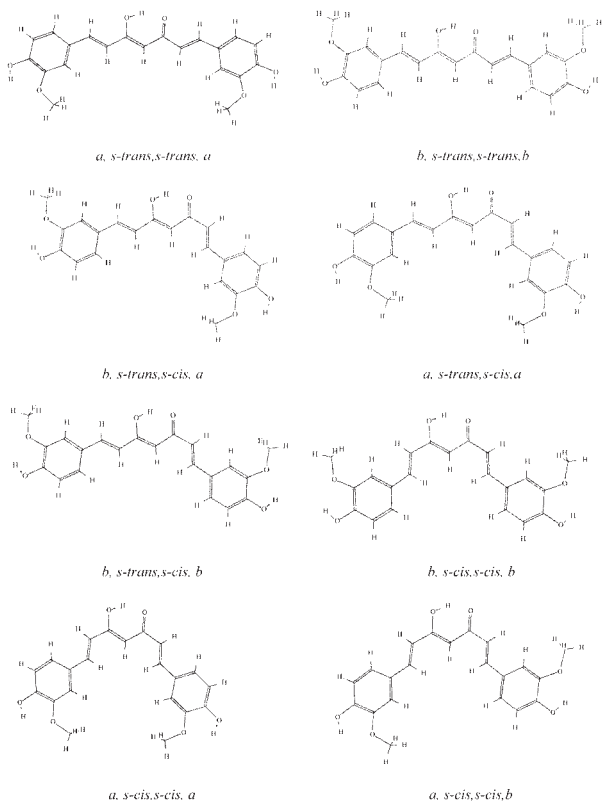

SCHEME 3. Some of more stable conformers of the curcumin–enol form.

TABLE II

Total and relative energies of some most stable conformers of curcumin.

Species	Total energy a.u.	VZPE kJ/mol	E_{rel} KJ/mol
1 *a, s-trans,s-trans, b*	−1263.5733482	976.546	0.00
2 *a, s-trans,s-trans, a*	−1263.5732766	976.441	0.083
3 *b, s-trans,s-trans, b*	−1263.5731275	976.662	0.695
4 *b, s-trans,s-cis, b*	−1263.5702179	976.373	8.046
5 *a, s-trans,s-cis, b*	−1263.5690966	976.036	10.653
6 *a, s-trans,s-cis, a*	−1263.5689952	976.085	10.968
7 *b, s-cis,s-cis, b*	−1263.5663044	975.341	17.288
8 *a, s-cis,s-cis, b*	−1263.5652466	975.196	19.921
9 *a, s-cis,s-cis, a*	−1263.5637719	975.066	23.663

MOLECULAR GEOMETRY

The optimized geometry parameters, i.e., bond lengths and bond angles, computed at the B3LYP/6-311G* level were compared with those found by single-crystal X-ray diffraction (Table III). According to the X-ray single crystal data, the curcumin molecules are linked by intermolecular hydrogen bonds between the hydroxyl group and O atoms of the enol group to form layers. Our calculations gave C_s(planar) geometry for curcumin with an intramolecular H-bond between neighboring OH and methoxy groups, and also O26-H47…O27. The calculated H-bond distance between O26…O27 is 2.54 Å. In the X-ray structure the same distance is 2.45 Å. Bearing in mind that in the crystal both O-atoms participate additionally in two intermolecular H-bonds, we consider that the computational method used gives very good results. One can see that the method used gives good descriptions of the geometry of the curcumin molecule. Our calculations

TABLE III

Theoretical (B3LYP/6-311G*) bond lengths (Å) and bond angles (degrees) compared with X-ray data of curcumin.

	B3LYP	Exp.		B3LYP	Exp.
Bonds			Bonds		
C^1—C^2	1.411	1.417	O^8—C^9	1.421	1.440
C^2—C^3	1.394	1.379	C^5—C^{10}	1.457	1.457
C^2—O^7	1.358	1.364	C^{10}—C^{11}	1.353	1.348
C^3—C^4	1.391	1.388	C^{11}—C^{12}	1.451	1.450
C^4—C^5	1.406	1.401	C^{12}—C^{13}	1.383	1.403
C^5—C^6	1.412	1.410	C^{13}—C^{14}	1.440	1.392
C^6—C^1	1.385	1.377	C^{12}—O^{26}	1.332	1.316
C^1—O^8	1.372	1.366	C^{14}—O^{27}	1.255	1.312
Angles			Angles		
$\angle(C^1C^2C^3)$	119.4	119.8	$\angle(C^4C^5C^6)$	118.1	118.9
$\angle(C^1C^2O^7)$	120.3	120.9	$\angle(C^6C^5C^{10})$	123.8	122.7
$\angle(C^1O^8C^9)$	118.5	116.7	$\angle(C^5C^{10}C^{11})$	127.9	128.3
$\angle(C^1C^6C^5)$	120.9	120.2	$\angle(C^{10}C^{11}C^{12})$	122.8	121.5
$\angle(C^2C^1C^6)$	120.1	120.5	$\angle(C^{11}C^{12}C^{13})$	122.1	121.7
$\angle(C^2C^1O^8)$	113.4	113.7	$\angle(C^{12}C^{13}C^{14})$	121.4	120.7
$\angle(C^2C^3C^4)$	120.3	120.0	$\angle(O^{26}C^{12}C^{13})$	121.5	119.9
$\angle(C^3C^4C^5)$	121.1	120.9	$\angle(O^{27}C^{14}C^{13})$	121.5	120.3

For atom numbering, see Scheme 1.

predict planar the E,E form for the isolated molecule, while in the crystal structure as a result of intermolecular H-bonding the molecule deviates from planarity. In that structure the oxygen atoms of the enol ring are engaged in intermolecular as well as in intramolecular hydrogen bonds. It may also be seen from the X-ray structure that there are no significant differences in the C—C in the skeleton or the C—O bonds in the enol ring. We computed the symmetric structure, which was closer to that determined by X-ray diffraction. According to our calculation, however, the symmetric structure should be by 15.4 kJ.mol^{-1} less stable than the asymmetric one. The calculations for the isolated molecule (gas phase) predicts C^{12}—O^{26} to be nearly single bond (1.332 Å), while C^{14}—O^{27} to be nearly double bond (1.225 Å) in character, respectively. The experimental values for the same bonds are 1.316 and 1.312 Å, respectively. The general trend for increasing the C—C single bond length and to decrease the C═C double bond lengths of the conjugated main backbone is presented. As can be seen in Table III, the bond length of C^{10}—C^{11}, C^{12}—C^{13}, C^{15}—C^{16} are close to the aromatic ones, while the single bonds C^{11}—C^{12}, C^{13}—C^{14}, C^{14}—C^{15} are shorter than the C—C single ones. The mean difference between the length of formal C—C and C═C bonds is defined as bond length alternation (BLA) [29]. In the studied molecule the values of BLA are about 0.07 Å. Similarly, bond length alternation was observed in the X-ray structure of curcumin [23]. BLA have been considered to be a crucial indicator for the performance of NLO-phores [30, 31]. Thus, on the molecular level, curcumin can be expected to exhibit NLO performance.

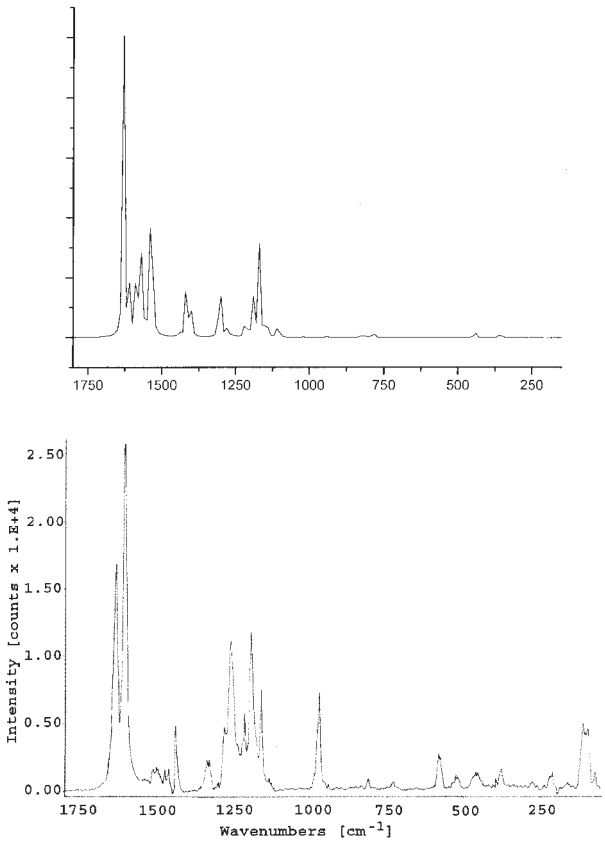

FIGURE 2. Theoretical (B3LYP/6-311 G*, up) and experimental Raman spectra (down) of curcumin.

VIBRATIONAL SPECTRA

Although the main subject of this study was to measure and interpret the experimental vibrational spectra of the curcumin molecule, we believe that it is useful to show the spectra obtained both in the solid state and in different solvents. The theoretical and experimental Raman spectrum in the solid state of curcumin is shown in Figure 2. The theoretical and experimental IR spectra, measured in KBr pellet and different solvents in the middle region, are compared in Figure 3. Examination of Figures 2 and 3 reveals that the experimental spectra of the studied compound are, in general, similar to that based on quantum chemical calculations for the isolated molecule. However, one cannot expect complete coincidence between experimental vibrational data and the theoretical data for the isolated molecule. The explanation for this difference is the effect of the hydrogen bonding interaction in the solid state spectra. Nevertheless, we used the computed vibrational data to determine the types of molecular motions associated with each of the observed experimental bands. The numerical values of the experimental vibrational frequencies and band intensities are listed with the theoretical ones in Table IV. The agreement between the calculated frequencies and the experimental data is very good. The mean absolute deviation ($a = n^{-1}\Sigma_i|\nu_i^{\mathrm{exp}} - \nu_i^{\mathrm{theor}}|$) between experimental ($\nu^{\mathrm{exp}}$) and theoretical ($\nu^{\mathrm{theor}}$) values is 8 cm^{-1}. It can be seen in Figure 3 that in the KBr pellet both phenolic ν(OH) vibrations have practically the same frequencies. The calculation supports this assignment and predicts, for both modes, frequencies of 3595 cm^{-1}. It is shifted downwards due to the intramolecular and intermolecular hydrogen bonds. The ν(OH) band, measured in carbon tetrachloride solution, is sharp at 3545 cm^{-1}. In $CDCl_3$ this band appears at 3536

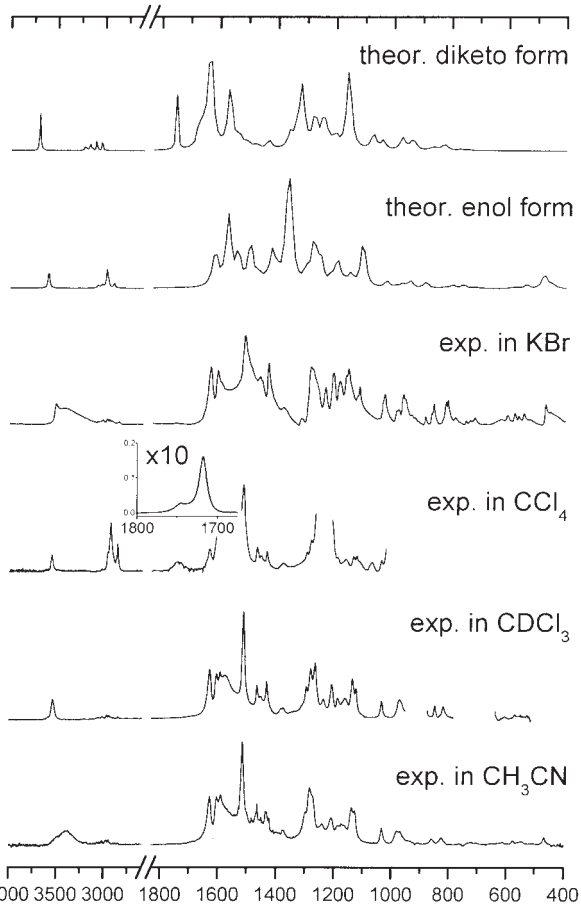

FIGURE 3. Theoretical (B3LYP/6-311G*) and experimental IR spectra of curcumin.

cm^{-1}. Finally, in acetonitrile solution this band is downshifted strongly to 3374 cm^{-1}, and it is strong and broad probably due to H-bonding between –OH groups and N-atoms of solvents. The enolic ν(OH) mode is predicted to be a strong band at 2979 cm^{-1}. No such band appears in either the IR or Raman spectra. The absence of a clearly defined ν(OH) band has been previously discussed by Tayyari et al. [32] and Chiavassa et al. [33] for similar compounds. The assignment of the experimental bands to the calculated normal modes in the C–H stretching region (3200–2700 cm^{-1}) is not obvious because there are fewer bands in the experimental spectrum than predicted by the calculations. The highest frequency experimental bands observed in the IR spectrum (3079–3000 cm^{-1}) are assigned to the aromatic C—H stretches, while the lower frequency bands are attributed to the methyl group motions. The ν(C—H) bands are of low intensity in both the experimental and theoretical spectra. For the diketo form, the theory predicts two modes associated with the C═O vibrations. The band at 1756 cm^{-1} with intensity 0.47 $km.mol^{-1}$ is assigned to symmetric C═O mode, while the band at 1732 cm^{-1} with intensity 211 $km.mol^{-1}$ corresponds to the asymmetric mode. So, the former band was ~450-fold weaker than the latter and could not be seen in the theoretical spectra within the scale used. We have found no bands in the carbonyl region (1800–1650 cm^{-1}) of experimental spectra in either the solid state or solutions. Only in the spectrum measured in tetrachlormethane in cells with a 5 mm pathlength are there bands at 1745 and 1717 cm^{-1} which can be assigned to asymmetric and symmetric ν(C═O) modes. The experimental vibrational data show that, in all cases, curcumin exists only in the *enol* form. Only in nonpolar CCl_4 does curcumin exist in a measurable amount of the diketo form. The NMR results [34] in $CDCl_3$ and DMSO also support the fact that the enol form is present in the solution by more that 90% in these solvents. In the discussion below we deal only with the assignment of the bands of the enol form of curcumin. The strong band at 1628 cm^{-1} (IR) and 1626 cm^{-1} (Raman) has a predominantly mixed ν(C═C) and ν(C═O) character. The frequency of this band is predicted well. The IR intensity is also calculated fairly well. It is difficult to explain explicitly why the strong Raman band, found experimentally at 1601 cm^{-1}, is predicted to be weak. We suppose in this case that the experimental 8a and 8b bands (Wilson's notation) are very close in frequency and their overlap produced one band of high intensity. This band is attributed to the mixed ν(C═O), ν(C═C) vibrational mode. The most prominent band in the IR spectrum is at 1510 cm^{-1}, while the corresponding Raman band at 1509 cm^{-1} is weak. These are attributed to highly mixed vibrations (Table IV). Deformation vibrations of the two methyl groups are pure. These were observed at 1460–1430 cm^{-1} and were calculated to be in the 1452–1420 cm^{-1} region. Most bands in frequency region 1450–1300 cm^{-1} are highly mixed. The bands at 1290 and 1282 cm^{-1} belong to the pure in-plane C—H vibrations of aromatic rings. The bands in 1277–1188 cm^{-1} are attributed to the in-plane deformation vibration of phenyl rings and skeletal in-plane deformations. The theory predicts well the frequencies of these vibrations and their intensities satisfactorily. It could be noted that in the abovementioned frequency region the vibrations of

TABLE IV

Experimental infrared (CsI pellet) and Raman (crystalline powder) and theoretical (B3LYP/6-311G*) spectral data of curcumin in frequency region 1800–600 cm^{-1}.

Assignment[a]	$\nu_{IR}^{exp.}$ [cm^{-1}]	$\nu_{Raman}^{exp.}$ [cm^{-1}]	$\nu^{calc.}$ [cm^{-1}]	$A_{IR}^{calc.}$ km · mol^{-1}	$A_{Raman}^{calc.}$ Å^4 · amu
$\nu_{C=C}$, $\nu_{C=O}$	1628	1626	1630	58.4	16997.1
$\nu_{C=O}$, $\nu_{C=C}$	1603	1601	1615	653.9	1049.9
$\nu_{CC}^{Ph(A)}$	1591		1587	31.5	3359.2
$\nu_{CC}^{Ph(B)}$			1586	23.3	1865.3
$\nu_{C=C}$, δ_{COH}^{enol}			1575	224.6	2543.5
$\nu_{CC}^{Ph(B)}$, δ_{COH}^{B}			1570	680.8	140.6
$\nu_{CC}^{Ph(A)}$, δ_{COH}^{A}			1568	489.3	4478.5
$\nu_{C=O}$, $\delta_{CC^{10}C}$, $\delta_{CC=O}$	1510	1509	1536	600.7	14888.1
$\delta_{CCH}^{Ph(B)}$, $\nu_{CC}^{Ph(B)}$		1497	1496	28.6	22.0
$\delta_{CCH}^{Ph(A)}$, $\nu_{CC}^{Ph(A)}$			1494	802.5	44.6
$\delta_{CH_3}^{A}$, $\delta_{CH_3}^{B}$	1471	1468	1466	25.0	2.8
$\delta_{CH_3}^{A}$, $\delta_{CH_3}^{B}$			1466	155.0	15.7
$\delta_{CH_3}^{A}$	1461		1452	9.7	22.3
$\delta_{CH_3}^{B}$	1457	1454	1452	9.2	21.9
$\delta_{CH_3}^{B}$			1441	67.7	158.6
$\delta_{CH_3}^{A}$			1440	16.3	8.0
δ_{CCC}^{Ph}, δ_{CCH}^{Ph}, δ_{COH}^{A}	1430	1431	1420	583.7	2162.5
δ_{CCC}^{Ph}, δ_{CCH}^{Ph}, δ_{COH}^{B}	1418		1409	4.4	111.7
$\delta_{C^{12}=CH}$	1413		1404	206.9	3468.7
δ_{COH}^{B}, δ_{COH}^{A}	1378		1368	1227.7	0.3
δ_{COH}^{enol} $\delta_{CCC}^{scel.}$	1374	1370	1368	67.7	0.3
δ_{COH}^{enol}, $\nu_{C=C}$, δ_{CCH}^{Ph}		1336	1357	1387.1	0.3
$\delta_{CC^{10}H}$, $\delta_{CC^{11}H}$, $\delta_{CCH}^{Ph(A)}$	1316	1321	1306	76.3	1946.6
δ_{C-Ph}, $\delta_{CCH}^{Ph(B)}$	1312	1312	1303	34.4	128.1
δ_{COH}^{enol}		1304	1301	143.8	1763.8
$\delta_{C=CH}$	1295		1284	45.1	194.6
$\delta_{C=CH}$, $\delta_{CCH}^{Ph(B)}$	1290		1280	3.7	110.4
$\delta_{C=CH}$, $\delta_{CCH}^{Ph(A)}$	1282		1276	812.7	572.0
$\delta_{CCH}^{Ph(B)}$, $\delta_{CCC}^{Ph(B)}$, δ_{COH}^{B}	1277	1273	1256	96.9	147.0
$\delta_{CCH}^{Ph(A)}$, δ_{COH}^{A}	1260	1256	1253	416.0	27.2
δ_{COH}^{B}, δ_{COH}^{A}, δ_{COH}^{enol}	1233	1230	1216	141.5	1434.7
$\delta_{CC^{11}H}$, $\delta_{CC^{15}H}$, δ_{CH_3}			1212	14.4	57.9
$\delta_{CCH}^{Ph(A)}$, $\delta_{CCH}^{scel.}$, δ_{CH_3}	1206	1207	1196	45.6	204.8
$\delta_{CCH}^{Ph(B)}$, $\delta_{CCH}^{scel.}$, δ_{CH_3}			1194	442.4	217.9
$\delta_{CCH}^{scel.}$			1188	15.2	2595.0
$\delta_{CH_3}^{B}$, $\delta_{CC^{16}H}$	1183	1184	1176	32.2	35.0
$\delta_{CH_3}^{A}$, δ_{COH}^{A}, $\delta_{CCH}^{scel.}$		1168	1169	59.1	5125.3
$\gamma_{CH_3}^{B}$, $\delta_{CCH}^{Ph(B)}$	1161		1150	131.0	1.3

(*Continued*)

TABLE IV
(Continued)

Assignment[a]	$\nu_{IR}^{exp.}$ [cm^{-1}]	$\nu_{Raman}^{exp.}$ [cm^{-1}]	$\nu^{calc.}$ [cm^{-1}]	$A_{IR}^{calc.}$ km · mol^{-1}	$A_{Raman}^{calc.}$ Å^4 · amu
$\delta_{CCH}^{Ph(A)}$, $\delta_{CCH}^{scel.}$	1153	1152	1145	90.1	1606.0
$\delta_{CCH}^{Ph(B)}$, $\nu_{O—CH_3}^{B}$		1138	1137	0.4	2.6
$\delta_{CCH}^{Ph(A)}$, $\nu_{O—CH_3}^{A}$			1137	0.6	3.8
$\delta_{CC^{15}H}$, $\delta_{CC^{13}H}$	1122	1120	1107	593.0	656.0
$\nu_{O—CH_3}^{A}$, $\delta_{CCH}^{Ph(A)}$,	1115	1116	1105	84.3	81.9
$\nu_{O—CH_3}^{B}$ $\delta_{CCH}^{Ph(B)}$, $\delta_{CC^{13}H}$			1104	230.7	96.8
$\delta_{CCH}^{Ph(B)}$, γ_{CH_3}	1033		1023	87.9	38.8
$\delta_{CCH}^{Ph(A)}$, γ_{CH_3}	1026		1022	30.8	12.7
$\gamma_{CC^{15}H}$, $\gamma_{CC^{16}H}$	988	985	989	29.1	2.5
$\gamma_{CC^{11}H}$, $\gamma_{CC^{10}H}$	978		971	34.1	3.0
$\delta_{CC^{13}H}$, $\nu_{C═O}$, $\delta_{CC^{15}H}$	966	967	966	37.6	27.6
$\nu_{C^{12}O}$, $\delta_{C^{12}OH}$	962	962	942	126.3	64.9
$\delta_{CCH}^{Ph(A)}$, $\delta_{CCC}^{Ph(A)}$, $\gamma_{CC^{10}H}$	933		915	0.9	1.5
$\delta_{CCH}^{Ph(B)}$, $\delta_{CCC}^{Ph(B)}$, $\gamma_{CC^{16}H}$	922		912	3.8	12.6
$\gamma_{CCH}^{Ph(B)}$, $\delta_{CCH}^{Ph(B)}$	906		896	1.2	0.9
$\gamma_{CCH}^{Ph(A)}$	886		895	0.7	0.7
γ_{COH}^{enol} $\nu_{C—O}^{enol}$		870	887	114.0	1.1
$\gamma_{CCH}^{scel.}$	864		862	0.9	5.0
$\gamma_{CCH}^{scel.}$, γ_{CCH}^{Ph}	856		856	0.9	1.4
$\gamma_{CCH}^{Ph(A)}$, $\gamma_{CCH}^{Ph(B)}$	831		828	0.7	67.1
$\gamma_{CCH}^{Ph(A)}$			824	10.0	11.0
$\gamma_{CCH}^{Ph(A)}$	814		815	7.7	92.5
$\gamma_{CCH}^{Ph(B)}$	808	809	795	27.3	1.1
$\gamma_{CCH}^{Ph(B)}$			793	14.3	0.9
$\gamma_{CCH}^{Ph(A)}$			793	16.3	25.0
γ_{CCH}^{Ph}	782		784	0.3	87.2
$\gamma_{CC^{13}H}$, $\gamma_{CC^{11}H}$, $\gamma_{CC^{15}H}$	767		757	62.7	7.1
$\gamma_{C^{2}OH}$, $\gamma_{CC^{13}H}$	744	744	748	5.4	4.6
$\gamma_{C^{2}OH}$, $\gamma_{CC^{12}H}$	729	726	716	13.9	0.8
δ_{CCH}^{Ph}, $\nu_{C═C}$, δ_{CCH}^{scel}	714	714	710	6.5	23.2
$\gamma_{CCH}^{Ph(A)}$, $\gamma_{CCC}^{Ph(A)}$			695	0.2	1.1
$\gamma_{CCH}^{Ph(B)}$, $\gamma_{CCC}^{Ph(B)}$	677		689	0.8	0.1
$\gamma_{CCH}^{scel.}$, $\gamma_{CCC}^{scel.}$	652		659	0.5	0.4

[a] Vibrational modes: ν, stretching; δ and γ, in-plane and out-of-plane bending, respectively; τ, torsion; superscript: Ph, aromatic ring vibrations; A, vibrations connected with 'enolic' part of the molecule (left); B, vibrations connected with the 'keto' part of the molecule (right).

phenyl group are strongly mixed with skeletal ones. The band at 886 cm^{-1}, belonging to the C—H out-of-plane vibration of aromatic rings, could be described as pure vibrations. The IR bands at 864 and 856 cm^{-1} are assigned to the highly mixed $\gamma_{C—H}$ and γ^{Ph}_{CCH}. Generally, the bands between 870 cm^{-1} and 710 cm^{-1} could be attributed to different C—H out-of-plane aromatic and skeletal motions. The weak bands at 534 (IR) and 530 cm^{-1} (Raman) were assigned to extremely complicated skeletal vibration, including out-of-plane deformations of the methyl and all OH groups. The deformation vibrations of both aromatic rings are in the frequency region 700–400 cm^{-1}. However, there are not pure, in most cases being mixed with γ^{scel}_{CCH} and δ^{scel}_{CCO}. The out-of-plane vibrations of both –OH groups are found at 438 cm^{-1} (IR), 440 cm^{-1} (Raman) are very well predicted at 442 cm^{-1}. The region of torsion vibrations is between 280 cm^{-1} and 50 cm^{-1}. The assignment of experimental bands below 120 cm^{-1} is difficult because of the absorption of the lattice modes in this region. The pure torsions are more predominant than mixed ones in this region.

Conclusions

The curcumin molecule in the crystal structure exists in enol form. According to the calculation (B3LYP/6-311G*) the *enol* form is more stable than *diketo*. The conformation of the more stable curcumin isomer practically coincides with that seen in the crystal structure. When it comes to curcumin enzyme interactions, many more conformational options are possible. In particular, the two enol-"carbonyl" oxygens present strong H-bond acceptors, and their specific interactions with suitable enzyme H-donor groups might well make accessible the enol *a,s-trans,s-trans-b* conformational space of curcumin to enzyme binding. The measured FTIR and Raman spectra in the solid state and in different solvents show that, in all cases, curcumin exists only in the *enol* form. Even in nonpolar solvents, such as CCl_4, the enol form predominates.

Our experimental and theoretical results show that the superb antioxidant activity may be due to the enol form, which gives the possibility for practically perfect conjugation between the two aromatic rings containing the active antioxidant centers.

References

1. Curcumin web site at URL http://www.curcuminoids.com.
2. Sharma, O. P. Biochem Pharmacol 1976, 25, 1811.
3. Masuda, T.; Toi, Y.; Bando, H.; Maekawa, T.; Takeda, Y.; Yamaguchi, H. J Agric Food Chem 2002, 50, 2524.
4. Mehta, K.; Pantazis, P.; McQueen, T.; Agarval, B. Anticancer Drugs 1987, 8, 471.
5. Nurfina, A. N.; Reksoha Diprodjo, M. S.; Timmerman, H.; Jenie, U.; Sigianto, D.; van der Goot, H. J Med Chem 1997, 32, 321.
6. Sreejayan, N.; Priyadarsini, K. I.; Devasagayam, A. T. P.; Rao, M. N. A. Int J Pharmacol 1997, 151, 125.
7. Venkatesan, P.; Rao, M. N. A. J Pharm Pharmacol 2000, 52, 1123.
8. Jankun, E.; McCabe, N.; Selman, Jankun, S. J. Int J Mal Med 2000, 6, 521.
9. Huang, M.; Lysz, T.; Ferraro, T.; Abidi, T.; Laskin, J.; Conney, A. Cancer Res 1991, 51, 813.
10. Ruby, A.; Kuttan, G.; Dinesh, B.; Rajasekaran, K.; Kuttan, K. Cancer Lett 1995, 94, 79.
11. Onoda, M.; Inano, H. Nitric Oxide 2000, 4, 505.
12. Gorman, A.; Hamblett, V.; Srinivasan, V.; Wood, P. Photochem Photobiol 1994, 59, 389.
13. Priyadarsini, K. Free Radic Biol Med 1997, 23, 838.
14. Priyadarsini, K.; Maity, D.; Naik, G.; Kumar, M.; Unnikrishnan, M.; Satav, J. ; Mohan, H. Free Radic Biol Med 2003, 35, 475.
15. Khopde, S.; Priyadarsini, K.; Ventkatesan, P.; Rao, M. N. A. Biophys Chem 1999, 80, 85.
16. Jovanovic, S. V.; Steenken, S.; Boone, C. W.; Simic, M. G. J Am Chem Soc 1999, 121, 9677.
17. Jovanovic, S. V.; Boone, C. W.; Steenken, S.; Trinoga, M.; Kaskej, R. B. J Am Chem Soc 2001, 123, 3064.
18. Bong, P-H. Bull Korean Chem Soc 2000, 21, 81.
19. Chignell, C.; Bilski, P.; Reszka, K.; Motten, A.; Sik, R.; Dahl, T. Photochem Photobiol 1994, 59, 295.
20. Miyamoto, M. Bull Chem Soc Jpn 1963, 36, 1208.
21. Tang, B.; Ma, L.; Wang, H.; Zhang, G. J Agric Food Chem 2002, 50, 1355.
22. Andreev, G. N.; Schrader, B.; Schulz, H.; Fuchs, R.; Popov, S.; Handjieva, N. Fresenius J Anal Chem 2001, 371, 1009.
23. Tønnesen, H. H.; Karlsen, J.; Mostad, A. Acta Chem Scand B 1982, 36,475.
24. Becke, A. D. J Chem Phys 1993, 98, 5648.
25. Lee, C.; Yang, W.; G. Parr, R. Phys Rev B 1988, 37, 785.
26. Scott A. P.; Radom, L. J Phys Chem 1996, 100, 16502.
27. Frisch, M. J.; Trucks, G. W.; Schlegel, H. B.; Scuseria, G. E.; Robb, M. A.; Cheeseman, J. R.; Zakrzewski, V. G.; Montgomery, J. A. , Jr.; Stratmann, R. E.; Burant, J. C.; Dapprich, S.; Millam, J. M.; Daniels, A. D.; Kudin, K. N.; Strain, M. C.; Farkas, O.; Tomasi, J.; Barone, V.; Cossi, M.; Cammi, R.; Mennucci, B.; Pomelli, C.; Adamo, C.; Clifford, S.; Ochterski, J.; Petersson, G. A;. Ayala, P. Y.; Cui, Q.; Morokuma, K.; Malick, D. K.; Rabuck, A. D.; Raghavachari, K.; Foresman,

J. B.; Cioslowski, J.; Ortiz, J. V.; Baboul, A. G.; Stefanov, B. B.; Liu, G.; Liashenko, A.; Piskorz, P.; Komaromi, I. ; Gomperts, R.; Martin, R. L.; Fox, D. J.; Keith, T.; Al-Laham, M. A.; Peng, C. Y.; Nanayakkara, A.; Gonzalez, C.; Challacombe, M.; Gill, P. M. W.; Johnson, B.; Chen, W.; Wong, M. W. ; Andres, J. L.; Gonzalez, C.; Head-Gordon, M.; Replogle E. S.; Pople, J. A. Gaussian 98, revision A.7; Gaussian, Inc.; Pittsburgh, PA, 1998.

28. Velcheva, E. A.; Stamboliyska, B. A. Spectrochim Acta 2003, 60, 2013.
29. Wolff; J.; Wortmann, R. In Advances in Physical Organic Chemistry, Vol. 32: Organic Materials for Second-Order Non-linear Optics; Bethell, D., Ed.; Academic Press: New York, 1999.
30. Gormann, C. B.; Marder, S. R. Chem Mater 1995, 7, 215.
31. Castiglioni, C.; Gussoni, M.; Del Zoppo, M.; Zerbi, G. Solid Sate Commun 1995, 82, 13.
32. Tayyari, S. F.; Zeegers-Huyskens, T.; Wood, J. L. Spectrochim Acta A 1979, 35, 1265.
33. Chiavassa, T.; Verlaque, P.; Pizzala, L.; Roubin, P. Spectrochim Acta A 1994, 50, 343.
34. Khopde, S. M.; Priyadarsini, K.; Palit D. K.; Mukherjee T. Photochem Photobiol 2000, 72, 625.